Structural, electronic, elastic, and piezoelectric properties of α -quartz and M X O 4 (M = Al , Ga, Fe; X = P , As) isomorph compounds: A DFT study

Pierre Labéguerie, Moussab Harb, Isabelle Baraille, Michel Rérat

Structural, electronic, elastic, and piezoelectric properties of α-quartz and MXO_4 (M=Al, Ga, Fe; X=P, As) isomorph compounds: A DFT study

Pierre Labéguerie, Moussab Harb, Isabelle Baraille, and Michel Rérat*

Institut Pluridisciplinaire de Recherche sur l'Environnement et les Matériaux, UMR CNRS 5254, Université de Pau et des Pays de l'Adour, Hélioparc Pau-Pyrénées, 2 Avenue du président Pierre Angot, 64053 Pau Cedex 9, France

(Received 22 July 2009; published 6 January 2010)

We report the structural, electronic, elastic, and piezoelectric properties of some α-quartz SiO_2 isotypes, namely, $AlPO_4$, $GaPO_4$, $GaAsO_4$, and $FePO_4$. This family of crystals is well known for its elastic and piezoelectric properties related to their MO_4 and XO_4 tetrahedral units, especially the M-O-X bridging angle θ and the tilt angle δ, the most distorted structures being expected to exhibit the highest piezoelectric coupling constant. We have then computed the optimized structure of each MXO_4 isomorph compound in order to study the variation in the elastic and piezoelectric tensors with respect to θ and δ. A comparison between our results at the density-functional theory level and the available data (theoretical and experimental ones) has been made. The differences observed for the whole class of systems has been discussed and a comparison with the SiO_2 α-quartz behavior is made.

DOI: 10.1103/PhysRevB.81.045107 PACS number(s): 71.10.−w, 71.20.Nr, 77.84.−s

I. INTRODUCTION

SiO_2 α quartz is a well-known piezoelectric crystal. MXO_4 (M=Al, Ga, Fe; X=P, As) type compounds derived from the SiO_2 α-quartz structure as other candidates have been widely studied due to their large amount of physical properties: optical activity, electro-optical effect, second-harmonic generation,…,[1–4] and of course piezoelectricity.[5–8]

High-pressure[9–12] and/or high-temperature[13–17] experiments have been reported in order to understand the transition between the existing crystalline forms or between crystalline and amorphous states; x-ray emission, optical method, ultraviolet photoelectron, and electron-energy loss[18] have been done to investigate the electronic structure; phonon spectrum and the related density of state were also measured,[19,20] etc.

Besides the piezoelectric effect is important and well known in this kind of systems, there still occurs some "limitations" that reduce the field of their potential applications, for example, pure α quartz, which is still one the most commonly used piezoelectric material, has limited performances at high temperature. This is one reason why the MXO_4 compounds have been studied so much, in order to get materials available beyond the actual α-quartz limits. A further possibility is to study the effect of variation in the chemical composition ($Al_xGa_{1-x}PO_4$, for example) on the piezoelectric behavior.[21–24]

Nowadays, it is well known[4,22,25,26] that the huge piezoelectric effect observed for that class of materials takes its origin in the structural distortion with respect to the β-quartz structure. Indeed, the most distorted structures are expected to exhibit the highest piezoelectric constants.[27] In fact, the distortion can be described by two interrelated angles. Effectively, the α-quartz structure consists in corner linked tetrahedra (Fig. 1), with the O atoms at the summits, and M or X atoms at the centers. In the α phase, these tetrahedra are tilted around the hexagonal a axes (Fig. 2).[25] This tilt angle, called δ, becomes zero at the α-β transition, vanishing the piezoelectric effect.[4] This δ angle is directly related to the intertetrahedral bridging angle θ. As pointed out by Haines *et al.*,[28] in the MXO_4 compounds case, the MO_4 and XO_4 tetrahedra have distinct tilt angles and two bridging angles due to the noncrystallographically equivalent oxygen atoms in the doubled unit cell.

The purpose of this work is to modelize the main physical skills of α-quartz homeotypes ($AlPO_4$, $GaPO_4$, $FePO_4$, and $GaAsO_4$) using the experience of our group in the study of structural, electronic, and vibrational[29,30] properties of crystals at the density-functional theory (DFT) level of theory and the recent implementation of the elastic and piezoelectric constants calculation in the CRYSTAL program.[31] After optimization of the geometries, we have compared the bond distances and angle values to the experimental ones. Then, we have computed the piezoelectric tensor and studied the influence of the tilt δ and bridging θ angles on its component values.

In order to complete this study, the corresponding elastic and dielectric tensors of MXO_4 have been also calculated and compared with the pure SiO_2 α quartz. The reliability with experimental values when available is also discussed.

This paper on the piezoelectric effect treated as the response of the material to the application of a strain tending to zero is a complementary work on the response of the α quartz to a strong electric field studied elsewhere.[32] The aim is to reproduce and analyze the experimental results of α-quartz materials when available and to provide a prediction of the studied quantities when no experimental data exist and give a starting point for further studies on the physical properties of solid solutions like $Al_xGa_{1-x}PO_4$, for example.

II. METHOD AND COMPUTATIONAL DETAILS

Calculations were performed with a standard version of the periodic *ab initio* CRYSTAL06 program.[31] Crystalline orbitals are linear combinations of Bloch functions (BF) and are evaluated over a regular three-dimensional mesh in reciprocal space. Each BF is built as a linear combinations of local atomic orbitals (AO), with a "phasis" factor in the re-

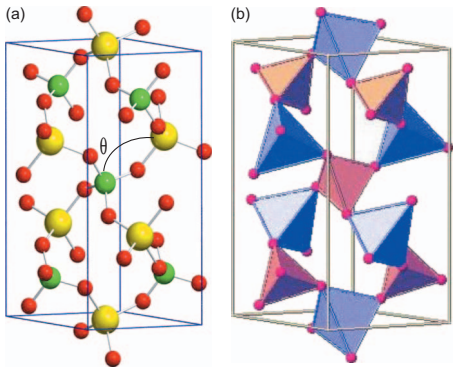

FIG. 1. (Color) The crystal structure of α-quartz homeotypes MXO_4. On the left hand (a), atomic representation with M (yellow), X (green), and O (red) positions as well as the M-O-X angle (θ). The corresponding tetrahedra are represented in (b) (MO_4 in blue and XO_4 in red).

ciprocal space. AO are contractions of Gaussian-type functions (GTF), each GTF being the product of a Gaussian function times a real solid spherical harmonic. All the electron basis sets used for Ga,[33] Al,[34] Fe,[35] P,[36] and O[37] atoms consist in 8-64111(41), 8-4111(1), 8-6411(41), 8-521(1), and 8-411(11) contractions, respectively. The exponents of the outer sp and d shells have been reoptimized at the B3LYP level to the following values (in bohr^{-2} units): $\alpha(\mathrm{Ga},sp)=\{0.663,0.175\}$, $\alpha(\mathrm{Ga},d)=0.669$; $\alpha(\mathrm{Al},sp)=\{0.600,0.389\}$, $\alpha(\mathrm{Al},d)=0.675$; $\alpha(\mathrm{Fe},sp)=\{0.543\}$, $\alpha(\mathrm{Fe},d)=0.392$; $\alpha(\mathrm{P},sp)=\{0.135\}$, $\alpha(\mathrm{P},d)=0.765$; and $\alpha(\mathrm{O},sp)=\{0.486,0.193\}$, $\alpha(\mathrm{O},d)=0.500$. The effective core potential of Durand and Barthelat[38] has been adopted for arsenic; PS-21(1) contractions of GTFs have been used for the valence electrons. The optimized exponents are $\alpha(\mathrm{As},sp)=\{0.130\}$, $\alpha(\mathrm{As},d)=0.263$.

Standard values for the computational tolerances as defined in the CRYSTAL06 manual[31] have been adopted for all steps of the calculation. In the geometry optimization, a structural relaxation procedure consisting of two independent steps was iteratively performed. In the first step, the cell parameters (a and c) are optimized with the atoms at fixed fractional positions. Cell optimization is carried out by means of a modified Polak-Ribiere algorithm in which the energy gradients are evaluated numerically by means of the central-difference formula.[39] In the second step, atomic positions are fully relaxed at fixed cell parameters. Forces on atoms are obtained by using the analytical DFT (Ref. 40) energy gradients and are used to relax the atoms to equilibrium by using a modified conjugate gradient algorithm proposed by Schlegel.[41] Convergence is tested on the rms and the absolute value of the largest component of the gradients and the estimated displacements. The threshold for the maximum force, the rms force, the maximum atomic displacement, and the rms atomic displacement on all atoms have been set to 0.00045, 0.00030, 0.00180, and 0.00120 a.u., respectively. The atomic position optimization is considered complete when these four conditions are satisfied. The crystal symmetry is maintained during the optimization process. The two-step structure optimization process is repeated until both the cell parameters and the atomic positions convergence criteria are satisfied.[42]

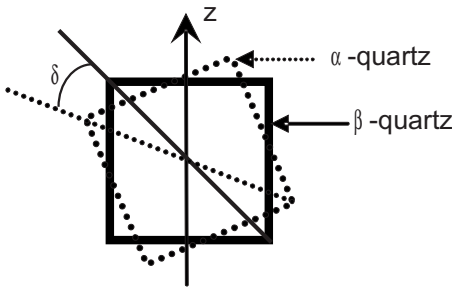

FIG. 2. Tilt angle, δ, related to the rotation angle between α-quartz and β-quartz structures.

Only the B3LYP (Becke's three-parameter exchange functional[43] and the nonlocal Lee-Yang-Parr correlation functional[44]) Hamiltonian form has been used. Previous studies[30,45] on elastic properties have shown that the hybrid functional gives slightly better results than the Hartree-Fock method and the generalized gradient approximation with respect to the experimental values while the local-density approximation approach overestimates the experimental data.

The details of the method, proposed by King-Smith and Vanderbilt,[46] and Resta[47] which is based on the Berry's phase, used here to compute the piezoelectric tensor have been described previously.[48–50] Since α-quartz-crystal structure is a trigonal $P3_121$ (or $P3_221$) space group, there are only two nonvanishing independent components of the elastic tensor, namely, e_{11} and e_{14}, the other components of the tensor being related to them as follow:

$$e_{11} = -e_{12} = -e_{16}/2, \tag{1}$$

$$e_{14} = -e_{25} \tag{2}$$

according to the notation given by Nye.[51]

Eleven η_i strain values in the [−0.020 and +0.020] interval were considered for the fitting. For each value of η_i, the three Berry's phase components φ_1, φ_2, and φ_3, corresponding to the phase differences of the state with and without strain in the three directions of the space (x, y, and z, respectively) are computed. During the deformation of the unit cell with a given strain, symmetry may be reduced and additional degrees of freedom must be fully relaxed.

A Taylor expansion of the unit-cell energy to second order as a function of the strain,

$$E(\eta) = E(0) + \sum_{i=1}^{6} \left[\frac{\partial E}{\partial \eta_i}\right]_0 \eta_i + \frac{1}{2}\sum_{i=1}^{6} \left[\frac{\partial^2 E}{\partial \eta_i \partial \eta_j}\right]_0 \eta_i \eta_j \tag{3}$$

has been considered for the calculation of the elastic constants. $E(0)$ stands for the energy of the equilibrium configuration and η_i refers to the strain components expressed according to Voigt's notation ($i=1,6$).

The elastic constants C_{ij} are related to the second derivatives of the energy with respect to strain components as follows:

TABLE I. Optimized unit-cell parameters (in Å), volume (in Å^3), and fractional atomic positions of the MXO_4 crystal. The percentage error compared to one of the experimental data are given in parenthesis.

	$AlPO_4$	$GaPO_4$	$FePO_4$	$GaAsO_4$	$AlPO_4$ [a]	$GaPO_4$ [b]	$FePO_4$ [c]	$GaAsO_4$ [d]
a	4.8966 (1%)	4.9793 (2%)	5.0032 (1%)	5.0755 (2%)	4.9438	4.89606	5.0362	4.9970
c	10.9047 (1%)	11.1556 (1%)	11.2075 (1%)	11.5475 (1%)	10.9498	11.02565	11.2554	11.3860
V	226.4 (3%)	239.5 (5%)	243.0 (2%)	257.6 (5%)	231.8	228.9	247.2	246.2
x_M	0.4606	0.4581	0.4487	0.4507	0.4665	0.4557	0.4583	0.4519
x_X	0.4593	0.4602	0.4548	0.4525	0.4669	0.4562	0.4577	0.4520
x_{O1}	0.4131	0.4080	0.4051	0.3972	0.4164	0.4103	0.4192	0.3855
y_{O1}	0.3047	0.3153	0.3303	0.3143	0.2919	0.3185	0.3181	0.3043
z_{O1}	0.3928	0.3925	0.3904	0.3832	0.2692	0.3925	0.3963	0.3888
x_{O2}	0.4111	0.4136	0.4117	0.4007	0.4155	0.4080	0.4131	0.4027
y_{O2}	0.2707	0.2714	0.2760	0.2934	0.2574	0.2717	0.2641	0.2926
z_{O2}	0.8781	0.8725	0.8680	0.8732	0.7829	0.8724	0.8749	0.8729

[a]Reference 16.
[b]Reference 8.
[c]Reference 52.
[d]Reference 27.

$$C_{ij} = \frac{1}{V_0}\left[\frac{\partial^2 E}{\partial \eta_i \partial \eta_j}\right]_0. \quad (4)$$

Energy second derivatives are evaluated numerically.

Since α-quartz-crystal structure is a trigonal $P3_121$ (or $P3_221$) space group, there are six nonvanishing independent components of the elastic tensor, namely, C_{11}, C_{12}, C_{13}, C_{14}, C_{33}, and C_{44}. As for the computation of the piezoelectric tensor, 11 η_i values in the [−0.020 and +0.020] interval were considered for the fitting. Once again, during the deformation of the unit cell with a given strain, symmetry may be reduced and additional degrees of freedom appear that must be fully relaxed.

III. RESULTS AND DISCUSSION

A. Optimized structure, θ and δ angles

The B3LYP optimized atomic positions and unit-cell parameters of $GaPO_4$, $GaAsO_4$, $AlPO_4$, and $FePO_4$, as well as the corresponding experimental data, are reported in Table I. A summary of the main interatomic bonds (namely, the M-O and X-O type links) and angles (O-M-O, O-X-O, and M-O-X) are given in Tables II and III, respectively. Concerning the specific case of the antiferromagnetic $FePO_4$ crystal,[53] a ferromagnetic state has been studied in order to lower the computational cost (a double supercell being necessary to modelize an antiferromagnetic spin configuration), the influence of the electronic spin configuration on the geometrical behavior of this compound being assumed to be negligible for our purpose.

The B3LYP Hamiltonian is known to give slightly overestimated but highly accurate results for the geometrical properties of crystalline systems. This assumption is confirmed here; the highest difference concerns the As-O computed distances in $GaAsO_4$ (≈3%). The relative error is larger on the unit-cell volume but it never exceeds 5% which is very acceptable. Concerning the bridging angles, all the values are smaller than the experimental data by less than 2%, except the M-O-P angles on $AlPO_4$ and $FePO_4$ compounds for which the underestimation is 4% and 5%, respectively. Our results are therefore in very good agreement with the available experimental data.

As previously observed,[54] the Al-O bond is the smallest M-O bond for that class of compounds, with an average value of 1.750 Å computed [1.735 (Ref. 16) and 1.726 (Ref.

TABLE II. Main distances (in Å) for each MXO_4 compound. The percentage error compared to one of the experimental data are given in parenthesis.

	$AlPO_4$	$GaPO_4$	$FePO_4$	$GaAsO_4$	$AlPO_4$ [a]	$GaPO_4$ [b]	$FePO_4$ [c]	$GaAsO_4$ [d]
$d_{M\text{-}O}$	1.748 (2%)	1.831 (2%)	1.884 (2%)	1.839 (1%)	1.730	1.804	1.850	1.823
	1.751 (1%)	1.840 (2%)	1.901 (3%)	1.849 (2%)	1.740	1.821	1.858	1.824
$d_{X\text{-}O}$	1.538 (2%)	1.544 (2%)	1.550 (2%)	1.700 (3%)	1.521	1.525	1.524	1.660
	1.539 (2%)	1.545 (2%)	1.550 (2%)	1.702 (3%)	1.523	1.526	1.529	1.662

[a]Reference 16.
[b]Reference 8.
[c]Reference 52.
[d]Reference 27.

TABLE III. Main angles (in °) for each MXO_4 compound.

	$AlPO_4$	$GaPO_4$	$FePO_4$	$GaAsO_4$	$AlPO_4$ [a]	$GaPO_4$ [b]	$FePO_4$ [c]	$GaAsO_4$ [d]
O-*M*-O	106.3	105.9	105.9	105.3	107.3	105.3	105.6	104.1
	110.0	109.6	109.4	108.8	109.2	110.3	109.0	108.3
	111.8	111.3	112.6	112.4	111.9	112.5	113.2	113.4
	112.6	114.6	113.8	112.8	111.9	113.3	114.7	114.5
O-*X*-O	108.4	108.0	107.3	106.7	108.3	107.5	108.5	104.6
	108.7	108.3	108.4	107.3	109.0	108.3	108.9	107.9
	109.4	109.9	110.1	110.2	109.1	109.7	109.9	108.3
	110.9	111.2	111.9	113.0	110.7	111.5	110.5	113.9
M-O-*X*	137.4	135.3	131.8	130.0	142.3	135.5	137.7	130.5
(θ)	138.3	135.2	132.6	129.9	142.6	134.3	139.0	130.4

[a]Reference 16.
[b]Reference 8.
[c]Reference 52.
[d]Reference 27.

55) Å experimentally] while the *M*-O bond is always above 1.80 Å for the rest of the materials. The largest bond length is observed in the $FePO_4$ system with an average value of 1.892 Å (1.854 Å experimentally[52]). We can therefore rank the *M*-O bonds depending on the corresponding system: $AlPO_4 < GaPO_4 < GaAsO_4 < FePO_4$. It corresponds exactly to the atomic size of the *M* atom: the atomic radius is 1.25, 1.30, and 1.40 Å for Al, Ga, and Fe, respectively.[56] The P atomic radius (1.00 Å) is also smaller than the As one (1.15 Å) but the difference is tight, and the *X* atom is not involved directly in the *M*-O bond, it is therefore logical that the Ga-O distances are quite similar in $GaPO_4$ and $GaAsO_4$.

The same trend is not observed for the *X*-O bond lengths. This is due to the large As-O distance of the $GaAsO_4$ compound while the average *X*-O link is around 1.54 Å in $AlPO_4$ (1.539 Å), $GaPO_4$ (1.545 Å), and $FePO_4$ (1.550 Å), it is close to 1.701 Å in the $GaAsO_4$ case. The replacement of the phosphorus atom by the arsenic one leads to a change (~0.15 Å) in the same order as the replacement of Al atom by Fe.

While the O-*M*-O and O-*X*-O angles are very close to the available experimental data, differences exist for θ=*M*-O-*X*. The experimental trend[1,25,54] for θ is $GaAsO_4 < GaPO_4 < FePO_4 < AlPO_4$, the exact opposite of the *X*-O bond-length one. In our calculations, we do not observe exactly this order, our average computed Fe-O-P value of 132.6° being smaller than the 138.4° value observed by Ng and Calvo.[52] They have linked the reduction in the Fe-O-P angle to the angular distortion of the FeO_4 tetrahedron. The same behavior is observed for the $AlPO_4$ crystal. Muraoka and Kihara[16] have studied the temperature dependence of the crystal structure of berlinite. According to their paper, the thermal vibrations might arise largely from the librational motions of the Al-O-P bonds around Al-P axes and from correlated translation motions of both the Al and P atoms along ⟨100⟩. They have also pointed out that the rotations of the XO_4 units around the twofold-symmetry axes are the main cause of the thermal expansion of α-quartz structure. This behavior is also present in $GaPO_4$ and $GaAsO_4$ but in a very smaller range, leading to more consistent results between theoretical (0 K) and experimental (room-temperature) values of the *M*-O-*X* angles.

The behavior of the piezoelectric effect in an α-quartz homeotype is linked to its θ and δ angles.[4,22,25] In our study, the average values of the θ angle are of 137.9°, 135.3°, 132.6°, and 130.0° for $AlPO_4$, $GaPO_4$, $FePO_4$, and $GaAsO_4$, respectively. Although theoretical results are computed at 0 K and not at room temperature, the use of the linear approximation between those two angles, given by[4,15,22,25]

$$\cos\theta = \frac{3}{4} - \left[\cos\delta + \frac{1}{2\sqrt{3}}\right]^2 \tag{5}$$

provides several important structural informations on the studied compounds. Furthermore, it allows us to understand more precisely the distortion occurring as regards to the α-β phase transition. The values of the δ tilt angle calculated from Eq. (5) lead to 21.2°, 23.1°, 25.4°, and 27.0° for $AlPO_4$, $GaPO_4$, $FePO_4$, and $GaAsO_4$, respectively. Philippot *et al.*[15] have measured these angles for a series of α-quartz compounds, including the later ones. Our results are in very good agreement with these measured angles for $GaPO_4$ (23.3° experimentally) and $GaAsO_4$ (26.2°) but differ for $AlPO_4$ (17.6°) and $FePO_4$ (21.5°). Obviously, we find again the discrepancy between our calculated values of the θ angle in $AlPO_4$ and $FePO_4$, and the experimental values.

Our theoretical results are consistent with the well-known experimentally empirical rule: for a considered α-quartz compound, an α-β phase transition is only possible when $\theta \geq 136°$ and $\delta \geq 22°$ at room temperature and pressure. Moreover, the same trend has been found concerning the (*M*-O)/(*X*-O) ratio, another experimental indication of the distortion of the structure: $GaAsO_4(1.08) < AlPO_4(1.14) < GaPO_4(1.20) < FePO_4(1.22)$.

To conclude, in spite of some differences between our results and the experimental data, the overall distortion trend leads to $GaAsO_4$ as the most promising compound to produce an important piezoelectric effect. Our computed piezo-

TABLE IV. Comparison between the theoretical and experimental values of direct gap (in eV) and optical dielectric constants.

	Direct gap (eV)		$\varepsilon_{xx}^{\infty}=\varepsilon_{yy}^{\infty}$		$\varepsilon_{zz}^{\infty}$	
	B3LYP	Expt.	B3LYP	Expt.	B3LYP	Expt.
SiO_2	8.77	9.2[a]	2.22	2.25[b]	2.26	2.27[b]
$AlPO_4$	8.61	8.0[c]	2.09	2.32[d]	2.15	2.35[d]
$GaPO_4$	7.11		2.35	2.57[e]	2.42	2.57[e]
$GaAsO_4$	5.68		2.57		2.67	
$FePO_4$	7.95 (up), 4.19 (down)		3.0		3.16	

[a]Reference 57.
[b]References 58 and 59 (obtained at $\lambda=300$ nm at 291 K).
[c]Reference 60.
[d]Reference 61.
[e]Reference 62.

electric constants, in particular, e_{14}, confirm this phenomenon (see Sec. III D).

B. Electronic properties: Direct gap and dielectric constants

In order to evaluate the electronic properties of these systems, the direct gap between the highest occupied molecular orbital and the lowest unoccupied molecular orbital, as well as the dielectric tensor have been computed. The calculated values are compared to the available experimental data in Table IV. Unfortunately, to our knowledge, only SiO_2 and $AlPO_4$ experimental values are available.[57,60] In the $FePO_4$ case, a distinction is made between the spin-up electronic gap and the spin-down one. For this compound, the sixtet ferromagnetic electronic spin configuration has been found 4.3 eV lower than the quartet or any other electronic spin configuration. Different behavior has been observed concerning our results while the gap is underestimated for SiO_2, it is overestimated for $AlPO_4$ (8.61 vs 8.0 eV).

The optical dielectric tensors have been determined using the finite field perturbation method.[63] For α-quartz structures, there are two independent dielectric constants $\in_{11}$ (equal to $\in_{22}$) and $\in_{33}$, the computed values are summarized in Table IV. The comparison can be made for SiO_2, $AlPO_4$, and $GaPO_4$ compounds; for SiO_2, we find 2.22 for $\in_{11}$ and 2.26 for $\in_{33}$, the experimental data being 2.25 and 2.27,[58,59] respectively. For $AlPO_4$ and $GaPO_4$, the computed values are smaller than the experimental ones, which may be linked to the overestimation of the direct gap. Both contributions increase from SiO_2 to $FePO_4$ following this tendency: $SiO_2 < AlPO_4 < GaPO_4 < GaAsO_4 < FePO_4$.

C. Elastic tensor

The α-quartz type of materials crystallize in the $P3_121$ or $P3_221$ space group, corresponding to a 32-point-group symmetry. This leads to an elastic tensor, written using the Voigt's contracted notation, build on six independent elastic constant,

$$[C_{ij}]=\begin{bmatrix} C_{11} & C_{12} & C_{13} & C_{14} & 0 & 0 \\ C_{12} & C_{11} & C_{13} & -C_{14} & 0 & 0 \\ C_{13} & C_{13} & C_{33} & 0 & 0 & 0 \\ C_{14} & -C_{14} & 0 & C_{44} & 0 & 0 \\ 0 & 0 & 0 & 0 & C_{44} & C_{14} \\ 0 & 0 & 0 & 0 & C_{14} & C_{66} \end{bmatrix}, \quad (6)$$

namely, C_{11}, C_{12}, C_{13}, C_{14}, C_{33}, and C_{44}. The C_{66} elastic constant is calculated from the C_{11} and C_{12} values using

$$C_{66}=(C_{11}-C_{12})/2 \quad (7)$$

while the off-diagonal component C_{12} is indirectly calculated using the C_{11} value which must be first obtained.

Due to the antiferromagnetic character[53] of the $FePO_4$ system, the theoretical computation of the elastic, as well as the piezoelectric properties of this compound is much more complex; this particular case will therefore be treated in a further work. The computed and experimental values of the six independent elastic constants for the considered crystals are reported in Table V. Unfortunately, to our knowledge except the experimental measurement of the C_{66} constant by Cambon *et al.*,[27] neither experimental nor theoretical data are available concerning $GaAsO_4$. Their value of 19.2 GPa is very close to ours (21.0 GPa).

Due to the difficulty of the experimental determination of the elastic constants, different experiences (on different samples) may lead to very different values. For example, the $AlPO_4$ experimental data are quite homogeneous for C_{11}, C_{44}, C_{14}, and C_{66}, the average values being 65.4, 43.1, −12.6, and 29.1 GPa, respectively. But some discrepancies exist on C_{33}, C_{12}, and C_{13}. The C_{33} value of Chang,[66] Sidek *et al.*,[67] and Bailey *et al.*[68] is found around 87.2 GPa while Wang *et al.*[65] have got a value of 55.8 GPa. The experimental data for C_{12} follows an increase trend from 2.3 GPa observed by Wang *et al.*,[65] to 10.5 GPa according to Bailey *et al.*[68] while Chang[66] and Sidek *et al.*[67] have obtained 7.2 and 9.0 GPa, respectively. The C_{13} contribution follows quite the same behavior: Wang *et al.*[65] value of 5.8 GPa is smaller than the

TABLE V. Theoretical and experimental values (in GPa) of the elastic constant of SiO_2 and the four MXO_4 α-quartz homeotypes.

	SiO_2		$AlPO_4$					$GaPO_4$					$FePO_4$		$GaAsO_4$
	B3LYP	Ref. 64	B3LYP	Ref. 65	Ref. 66	Ref. 67	Ref. 68	B3LYP	Ref. 69	Ref. 70	Ref. 71	Ref. 72	Regres.	Ref. 73	B3LYP
C_{11}	***89.7***	86.8	***87.9***	63.4	64.0	64.9	69.3	***74.6***	66.6	70.7	66.7	66.37	*72.8*	37.7[b]	***60.7***
C_{33}	***112.0***	105.8	***122.4***	55.8	85.8	87.1	88.6	***100.7***	102.1	58.3	103.8	103.29	*96.2*	85.3[b]	***95.4***
C_{44}	***57.9***	58.2	***43.3***	43.1	43.2	43.1	43.0	***44.6***	37.7	41.9	62.5	37.85	*41.3*	18.7[b]	***28.1***
C_{12}	***12.8***	7.0	***27.1***	2.3	7.2	9.0	10.5	***24.0***	21.8	6.6	−12.9	(21.5)[b]	*22.7*	18.2[b]	***18.6***
C_{13}	***16.4***	11.9	***30.4***	5.8	9.6	14.6	13.5	***27.0***	24.9	6.6	−22.5		*26.3*	18.6[b]	***22.7***
C_{14}	***−14.8***	−18.1	***−11.2***	−12.1	−12.4	−12.7	−13.0	***4.7***	3.9	17.8	3.5	4.93	*3.8*	12.2[b]	***3.12***
C_{66}	***38.5***	39.9	***30.4***	30.6	28.4	27.9	29.4	***25.3***	(22.4)[a]	(32.1)[a]	(39.8)[a]	22.46	*25.0*	9.7[b]	***21.0***

[a]Calculated using the relation $C_{66}=(C_{11}-C_{12})/2$.

[b]Calculated from the slopes of the acoustic phonon branches near the Brillouin-zone center.

Chang[66] one (9.6 GPa), Sidek *et al.*[67] and Bailey *et al.*[68] give almost the same value (14.6 and 13.5 GPa, respectively). An accurate theoretical calculation of these components may therefore help to understand the reasons of such differences or at least provide some informations on the expected values.

The elastic constants computed at the B3LYP level for $AlPO_4$ can be classified into three classes: (1) The values are in very good agreement with the experimental data, which is the case for the C_{44}, C_{14}, and C_{66} constants with the best experimental homogeneity. (2) The C_{11} and C_{33} values are overestimated by 34% and 29%, respectively, respected to the average experimental data. (3) None of our indirect results for C_{12} and C_{13} is particularly close to experimental data; we found C_{12} (27.1 GPa) and C_{13} (30.4 GPa) constants larger than the experimental trend, due probably to the overestimation of C_{11} and C_{33}.

The $GaPO_4$ case is a bit more complex due to the large discrepancy between all the experimental data. For example, in the four typical experimental works considered here,[69–72] the C_{12} is not reported in Ref. 72, Huard[71] observed a negative value, Engel *et al.*[70] have got only +6.6 GPa while Wallnöfer *et al.*[69] obtained +24.87 GPa. If we calculate, the C_{12} contribution of Armand *et al.*[72] using their values of C_{11} and C_{66}, we obtain a C_{12} elastic constant of 21.5 GPa, in very good agreement with our results (27.0 GPa) and Wallnöfer's ones. For C_{11}, even if Engel *et al.*[70] gave a slightly larger value than the rest of the experimental data (70.7 vs around 66.6 GPa), our value (74.6 GPa) is in good agreement with experiment. The calculated C_{33}, C_{14}, and C_{66} constants are in very good agreement with the experimental data: except for the low value of Engel[70] (58.3 GPa), the computed C_{33} value (100.7 GPa) is very close to the experimental results [102.1 (Ref. 69), 103.8 (Ref. 71), and 103.3 (Ref. 72) GPa]; also our value obtained for C_{14} (4.7 GPa) is in very good agreement with the experimental ones[69,71,72] (3.9, 3.5, and 4.9 GPa, respectively) that of Engel *et al.*[70] being much larger (17.8 GPa). At last, only Armand *et al.*[72] have measured directly the C_{66} contribution (22.5 GPa), which is close to our result (25.3 GPa). The C_{66} contribution according to relation (7) leads to 22.4 GPa from the C_{11} and C_{12} Wallnöfer's values,[69] in good agreement with ours and that of Armand *et al.*[72] while those of Engel *et al.*[70] (32.1 GPa) and Huard[71] (39.8 GPa) are overestimated. For the C_{44} elastic constant, Huard's measure (62.5 GPa) (Ref. 71) is larger than the other experimental [37.7,[69] 37.9,[72] and 41.9 (Ref. 70) GPa] and our theoretical (44.6 GPa) results.

Despite the lack of experimental measurements for $GaAsO_4$, it is still possible to analyze the theoretical results with those of the $AlPO_4$ and $GaPO_4$ systems. Except for the C_{44} contribution, for which the $GaPO_4$ computed value is slightly larger than the $AlPO_4$ one (44.6 vs 43.3 GPa), the computed elastic constant of $AlPO_4$ are larger than the $GaPO_4$ ones, which are larger than the $GaAsO_4$ values. This is obviously due to the volume of the unit cell, the bigger is the cell the smaller are the elastic constants. Indeed, as mentioned in the computational details, the elastic constant calculation is based on the second derivative of the energy divided by the unit-cell volume. The elastic constant value as a function of the unit-cell volume is reported on Fig. 3. Except for C_{11} and C_{33} for which a second-order polynomial fit has been used, the other elastic constants are strictly linearly dependent of the volume. Based on this tendency, a prediction of the $FePO_4$ elastic tensor could be made (the volume of the unit cell being 243.0 Å^3), leading to the values reported in Table V. They largely differ from the elastic constant calcu-

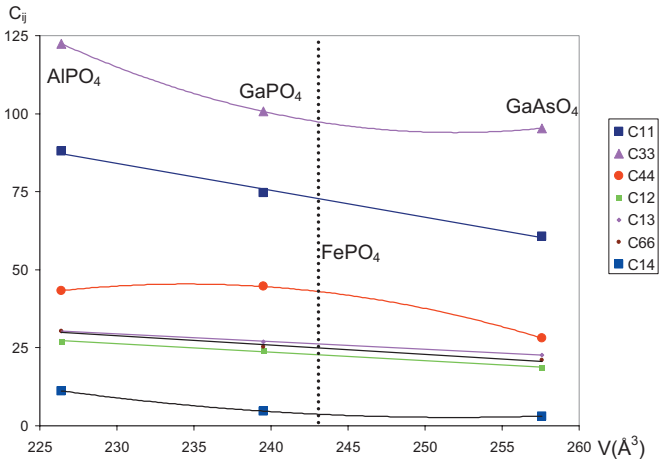

FIG. 3. (Color) Elastic constants (in GPa) as a function of the unit-cell volume (in Å^3). The dash line represents the volume calculated for $FePO_4$.

TABLE VI. Theoretical and experimental values (in C/m^2) of the piezoelectric constant of SiO_2 and the four MXO_4 α-quartz homeotypes.

	SiO_2 Si-O-Si=143° (tilt angle δ=17°)		$AlPO_4$ Al-O-P=137.9° (δ=21.2°)				$GaPO_4$ Ga-O-P=135.3° (δ=23.1°)		$GaAsO_4$ Ga-O-As=130.0° (δ=27.0°)
	B3LYP	Ref. 64	B3LYP	Ref. 65	Ref. 66	Ref. 15	B3LYP	Ref. 69	B3LYP
e_{11}	***0.18***	0.172	***0.20***	0.22[a]	0.30[a]	0.16[a]	***0.22***	0.21[a]	***0.20***
e_{14}	***−0.06***	−0.039	***−0.05***	−0.15 [a]	−0.13 [a]	−0.01 [a]	***0.08***	0.11[a]	***0.17***

[a]Calculated from the relation $e_{ik}=\Sigma_{j=1}^{6} d_{ij}c_{jk}$, where d_{ij} and c_{ij} are determined experimentally.

lated by Mittal *et al.*[73] from the slopes of the acoustic phonon branches near the Brillouin-zone center.

D. Piezoelectric tensor

Due to the important piezoelectric character of MXO_4 (M=Al, Ga, Fe; X=P, As) compounds, many studies[3,4,7,23,27,28,72,74] have been carried out to determine, analyze, understand, and eventually improve their response property to a strain or an electric field. In particular, the reliability under pressure, temperature and/or composition variation is a major subject in piezoelectric material research.

The precise and reliable computation of such properties at the theoretical level using a first-principle approach has been a real challenge for many years. One of the latest approach proposed to solve this problem is the quantum-mechanical theory based on the Berry phases, presented by King-Smith and Vanderbilt,[46] and Resta.[47] In particular, this method which has been implemented in the CRYSTAL program,[31] avoids some of the problems linked to the definition of the polarization in periodic systems.[75]

In α-quartz type compounds, only two independent constants are necessary to build this tensor. Indeed, the piezoelectric tensor can be written as

$$[e_{ij}] = \begin{bmatrix} e_{11} & -e_{11} & 0 & e_{14} & 0 & 0 \\ 0 & 0 & 0 & 0 & -e_{14} & -2e_{11} \\ 0 & 0 & 0 & 0 & 0 & 0 \end{bmatrix}. \quad (8)$$

The properties $e_{ij}=-(\frac{\partial P_i}{\partial \eta_j})_{E=0}$ are derived from the direct computation of the variation in the intensity of the polarization P_i (Voigt's notation) in the i direction induced by the application a strain η_j in the j direction while the experimental measurement is based on the application of an electric field, leading to a piezoelectric strain coefficients d_{ij} response, defined as the variation in the strain η_j in terms of the variation in the applied electric field E_i,

$$d_{ij} = -\left(\frac{\partial \eta_j}{\partial E_i}\right)_{\tau=0}, \quad (9)$$

where τ is the stress component. The direct comparison of the experimental and theoretical values is therefore impossible. Nevertheless, it is possible to calculate one quantity knowing the other one. To get the d_{ij} contribution knowing the e_{ij} one, the S_{ij} elastic compliance coefficients have to be determined via the thermodynamical relation,

$$d_{ij} = \sum_{k=1}^{6} e_{ik}S_{kj}. \quad (10)$$

In order to avoid the accumulation of computational errors and to use in priority experimental data, we have converted the available d_{ij} measurement into e_{ij} contribution,

$$e_{ij} = \sum_{k=1}^{6} d_{ik}C_{kj} \quad (11)$$

using the experimental elastic constants C_{ij} usually presented in the same experimental work. In the α-quartz structure, this leads to

$$e_{11} = d_{11}(C_{11} - C_{12}) + d_{14}C_{14} \quad (12)$$

and

$$e_{14} = 2d_{11}C_{14} + d_{14}C_{44}. \quad (13)$$

The computed values as well as the "calculated" experimental data are reported in Table VI. As mentioned before, $FePO_4$ being more complicated than the other compounds due to its antiferromagnetic behavior, the piezoelectric tensor has not been computed yet.

The agreement between the B3LYP results and experimental data is very good, the biggest difference concerns the e_{14} piezoelectric constant of $AlPO_4$ for which −0.05 C/m^2 is obtained with B3LYP while −0.15 and −0.13 C/m^2 are the experimental values obtained by Wang *et al.*[65] and Chang.[66] The value obtained by Philippot *et al.*[15] is closer to ours. This difference is due to the sum of imprecision needed to compare theoretical and experimental value as well as the strong temperature effect on the elastic constants. Nevertheless, this difference is acceptable, the e_{14} piezoelectric constant value being very small.

Concerning the e_{11} contribution, we observe that for each considered compounds $AlPO_4$, $GaPO_4$, and $GaAsO_4$, the corresponding value is around 0.2 C/m^2 (0.20, 0.22, and 0.20 C/m^2, respectively). It appears that the structural deformation of the structure of this type of materials does not affect the e_{11} contribution to the piezoelectric effect. In fact, the variation in the d_{11} piezoelectric "strain" constant observed experimentally is compensated by the elasticity of the unit cell (C_{11}, for example), the former increases from $AlPO_4$ to $GaAsO_4$ ($AlPO_4 < GaPO_4 < FePO_4 < GaAsO_4$) while the latter decreases in the same trend, leading to an apparently stable e_{11} piezoelectric "polarized" constant.

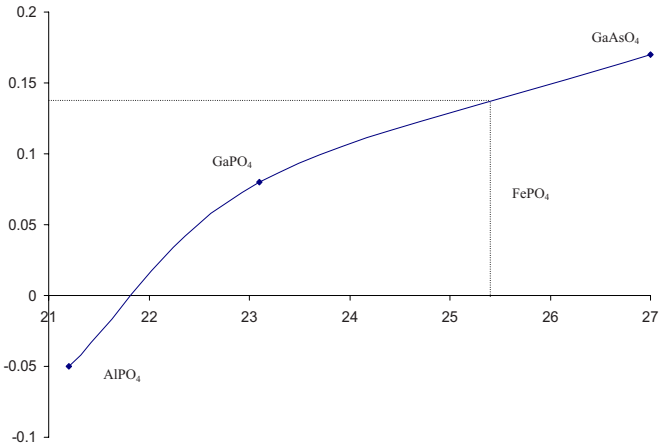

FIG. 4. (Color online) Piezoelectric constant e_{14} (in C/m^2) as a function of the tilt angle δ (in degrees).

This phenomenon is not observed in the e_{14} case. Indeed, the e_{14} contribution seems to be directly linked to the distortion of the material: if we classified the compounds in terms of their δ tilt angle [or reversely to their M-O-P angle(θ)]: $AlPO_4 < GaPO_4 (< FePO_4) < GaAsO_4$, we get the same trend for the e_{14} piezoelectric constants $-0.05 < 0.08 < 0.17$ C/m^2, respectively (cf. Fig. 4). This leads to a change in the relative sign of e_{14} compared to e_{11} while it is negative for $AlPO_4$ (due to the negative value of the C_{14} elastic constant), it becomes positive in $GaPO_4$ and $GaAsO_4$.

Consequently, we assume $FePO_4$ to exhibit a d_{ij} piezoelectric strain constant between $GaPO_4$ and $GaAsO_4$ value, an e_{11} contribution close to 0.2 C/m^2 and an e_{14} constant around 0.3 C/m^2 ($0.08 < e_{14} < 0.17$ C/m^2). Second order polynomial regression based on our calculations (e_{14} piezoelectric constant and the corresponding tilt angle) gives an e_{14} value of 0.14 C/m^2 for a tilt angle δ of 25.4° for $FePO_4$.

As expected, the more distorted $GaAsO_4$ system in terms of θ angle, δ tilt angle and (M-O)/(X-O) ratio corresponds to the strongest piezoelectric behavior (cf. Fig. 4).

IV. CONCLUSION

The piezoelectric effect is defined as the influence of an electric field on material whose response is a deformation of its structure or, conversely, the apparition of an internal electric polarization in the crystal due to the application of a determinate strain. As described in Sec. III D, the method implemented in the CRYSTAL (Ref. 31) code that has been used in this study is based on the second definition of the piezoelectric effect while the experimental measurement is based on the first one. The simulation of the experimentally observed displacement and/or rotation therefore improves our fundamental understanding of this specific physical property. For this purpose, the response of SiO_2 α quartz to a strong electric field is studied in a complementary work using the same finite field perturbation method than previously for the dielectric constant determination.[32]

The present work compares the elastic and piezoelectric properties of SiO_2 and α-quartz homeotypes MXO_4 largely studied previously at the experimental level. To our knowledge, it is the first theoretical study of these properties with respect to the geometry, which gives complementary information on the physical properties of these materials.

Concerning the elastic tensor calculation, the results obtained at the B3LYP level are in good agreement with experiment except for some off-diagonal components particularly. One should notice that the trend observed previously for the values of the elastic constants of α-quartz systems in terms of unit-cell volume is confirmed if a double unit-cell system for SiO_2 is considered.

The piezoelectric tensors calculated at the B3LYP level are in good agreement with the experimental measurement made by Kushibiki *et al.*[64] The SiO_2 e_{11} value is consistent with the 0.2 C/m^2 trend observed in the α-quartz homeotype. Again, the 143° value obtained for the Si-O-Si angle leads to a negative e_{14} value lower than the $AlPO_4$ one, the largest θ angle leading to the lowest e_{14} piezoelectric contribution.

Finally, the relationship between the structural distortion and the piezoelectric behavior has been confirmed theoretically. In particular, the effect of the value of the θ angle or the corresponding δ tilt angle has been proven. This fair agreement between the calculated values and the experimental available data reinforces the predicted values for $GaAsO_4$ and $FePO_4$ for which a lack of experimental results is observed.

*Corresponding author; michel.rerat@univ-pau.fr

[1] K. Kosten and H. Arnol, Z. Kristallogr. **152**, 119 (1980).
[2] D. L. Lakshtanov, S. V. Sinogeikin, and J. D. Bass, Phys. Chem. Miner. **34**, 11 (2006).
[3] H. Ribes, J. C. Giuntini, A. Goiffon, and E. Philippot, Eur. J. Solid State Inorg. Chem. **25**, 201 (1988).
[4] P. W. Krempl, J. Phys. IV **126**, 95 (2005).
[5] A. Goullet, J. Pascual, R. Cusco, and J. Camassel, Phys. Rev. B **44**, 9936 (1991).
[6] J. D. Foulon, J. C. Giuntini, and E. Philippot, Eur. J. Solid State Inorg. Chem. **31**, 245 (1994).
[7] H. Ogi, T. Ohmori, N. Nakamura, and M. Hirao, J. Appl. Phys. **100**, 053511 (2006).
[8] J. Haines, O. Cambon, N. Prudhomme, G. Fraysse, D. A. Keen, L. C. Chapon, and M. G. Tucker, Phys. Rev. B **73**, 014103 (2006).
[9] H. Sowa, Z. Kristallogr. **209**, 954 (1994).
[10] S. M. Clark, A. G. Christy, R. Jones, J. Chen, J. M. Thomas, and G. N. Greaves, Phys. Rev. B **51**, 38 (1995).
[11] M. J. Peters, M. Grimsditch, and A. Polian, Solid State Commun. **114**, 335 (2000).
[12] W. Duan, R. M. Wentzcovitch, and J. R. Chelikowsky, Phys. Rev. B **60**, 3751 (1999).
[13] H. Nakae, K. Kihara, and M. Okuno, Z. Kristallogr. **210**, 746 (1995).
[14] O. Baumgartner, A. Preisinger, P. W. Krempl, and H. Mang, Z.

Kristallogr. **168**, 83 (1984).
[15] E. Philippot, D. Palmier, M. Pintard, and A. Goiffron, J. Solid State Chem. **123**, 1 (1996).
[16] Y. Muraoka and K. Kihara, Phys. Chem. Miner. **24**, 243 (1997).
[17] J. Haines and O. Cambon, Z. Kristallogr. **219**, 314 (2004).
[18] A. Di Pomponio, A. Continenza, L. Lozzi, M. Passacantando, S. Santucci, and P. Picozzi, Solid State Commun. **95**, 313 (1995).
[19] D. M. Christie and J. R. Chelikowsky, J. Phys. Chem. Solids **59**, 617 (1998).
[20] W. Dultz, M. Quilichini, J. F. Scott, and G. Lehmann, Phys. Rev. B **11**, 1648 (1975).
[21] R. Mittal, S. L. Chaplot, and N. Choudhury, Prog. Mater. Sci. **51**, 211 (2006).
[22] J. Haines, O. Cambon, D. Cachau-Herreillat, G. Fraysse, and F. E. Mallassagne, Solid State Sci. **6**, 995 (2004).
[23] S. N. Achary, A. K. Tyagi, P. S. R. Krishna, A. B. Shinde, O. D. Jayakumar, and S. K. Kulshresththa, Mater. Sci. Eng., B **123**, 149 (2005).
[24] S. N. Achary, R. Mishra, O. D. Jayakumar, S. K. Kulshreshtha, and A. K. Tyagi, J. Solid State Chem. **180**, 84 (2007).
[25] E. Philippot, P. Armand, P. Yot, O. Cambon, A. Goiffon, G. J. McIntyre, and P. Bordet, J. Solid State Chem. **146**, 114 (1999).
[26] P. Worsch, B. Koppelhuber-Bitschnau, F. A. Mautner, P. W. Krempl, and W. Wallnöfer, Mater. Sci. Forum **600**, 278 (1998).
[27] O. Cambon, J. Haines, G. Fraysse, J. Détaint, B. Capelle, and A. Van der Lee, J. Appl. Phys. **97**, 074110 (2005).
[28] J. Haines, O. Cambon, J. Rouquette, V. Bornand, Ph. Papet, J. M. Léger, and S. Hull, Mater. Sci. Forum **277**, 443 (2004).
[29] M. Mérawa, P. Labéguerie, P. Ugliengo, K. Doll, and R. Dovesi, Chem. Phys. Lett. **387**, 453 (2004).
[30] P. Labéguerie, F. Pascale, M. Mérawa, C. Zicovich-Wilson, N. Makhouki, and R. Dovesi, Eur. Phys. J. B **43**, 453 (2005).
[31] V. R. Saunders, R. Dovesi, C. Roetti, R. Orlando, C. M. Zicovich-Wilson, F. Pascale, N. M. Harrison, K. Doll, B. Civalleri, I. J. Bush, P. D'Arco, and M. Llunell, in CRYSTAL06 User's Manual (University of Torino, Torino, 2006).
[32] M. Harb, P. Labéguerie, I. Baraille, and M. Rérat, Phys. Rev. B **80**, 235131 (2009).
[33] R. Pandey, M. Causa, N. M. Harrison, and M. Seel, J. Phys.: Condens. Matter **8**, 3993 (1996).
[34] M. Catti, G. Valerio, R. Dovesi, and M. Causà, Phys. Rev. B **49**, 14179 (1994).
[35] M. Catti, G. Valerio, and R. Dovesi, Phys. Rev. B **51**, 7441 (1995).
[36] C. M. Zicovich-Wilson, A. Bert, C. Roetti, R. Dovesi, and V. R. Saunders, J. Chem. Phys. **116**, 1120 (2002).
[37] F. Corà, Mol. Phys. **103**, 2483 (2005).
[38] P. Durand and J. C. Barthelat, Theor. Chim. Acta **38**, 283 (1975).
[39] C. M. Zicovich-Wilson, LoptCG Shell procedure for numerical gradient optimization, Universidad Autonoma del Estado de Morelos, Mexico, 1998.
[40] R. Orlando, V. R. Saunders, R. Dovesi (unpublished).
[41] H. B. Schlegel, J. Comput. Chem. **3**, 214 (1982).
[42] B. Civalleri, Ph. D'Arco, R. Orlando, V. R. Saunders, and R. Dovesi, Chem. Phys. Lett. **348**, 131 (2001).
[43] A. D. Becke, J. Chem. Phys. **98**, 5648 (1993).
[44] C. Lee, W. Yang, and R. G. Parr, Phys. Rev. B **37**, 785 (1988).
[45] M. Mérawa, Y. Noël, B. Civalleri, R. Brown, and R. Dovesi, J. Phys.: Condens. Matter **17**, 535 (2005).
[46] R. D. King-Smith and D. Vanderbilt, Phys. Rev. B **47**, 1651 (1993).
[47] R. Resta, Rev. Mod. Phys. **66**, 899 (1994).
[48] M. Catti, Y. Noël, and R. Dovesi, J. Phys.: Condens. Matter **17**, 4833 (2005).
[49] Y. Noel, M. Catti, and R. Dovesi, Ferroelectrics **300**, 139 (2004).
[50] P. Labéguerie, Ph.D. thesis, Université de Pau et des Pays de l'Adour, 2005.
[51] J. F. Nye, *Physical Properties of Crystal: Their Representation by Tensors and Matrices*, 2nd ed. (Oxford University Press, New York, 1985).
[52] H. N. Ng and C. Calvo, Can. J. Chem. **53**, 2064 (1975).
[53] V. Beckmann, W. Bruckner, W. Fuchs, G. Ritter, and H. Wegener, Phys. Status Solidi **29**, 781 (1968).
[54] A. Goiffon, J. C. Jumas, M. Maurin, and E. Philippot, J. Solid State Chem. **61**, 384 (1986).
[55] N. Thong and D. Schwarzenbach, Acta Crystallogr., Sect. A: Cryst. Phys., Diffr., Theor. Gen. Crystallogr. **35**, 658 (1979).
[56] M. Bernard and F. Busnot, *Usuel de Chimie Générale et Minérale* (Dunod, Paris, 1996).
[57] D. W. McComb and A. Howie, Nucl. Instrum. Methods Phys. Res. B **96**, 569 (1995).
[58] D. N. Nikogosyan, *Properties of Optical and Laser-Related Materials: a Handbook* (Wiley, New York, 1997).
[59] R. B. Sosman, *The Properties of Silica* (Chemical Catalog Company, New York, 1927).
[60] T. H. Distefano and D. E. Eastman, Solid State Commun. **9**, 2259 (1971).
[61] M. J. Weber, *Handbook of Laser Science and Technology* (CRC, Cleveland, 1995), Vol. 2.
[62] A. I. Motchany, P. P. Chvanski, and N. I. Leonyuk, Prog. Cryst. Growth Charact. Mater. **40**, 243 (2000).
[63] C. Darrigan, M. Rérat, G. Mallia, and R. Dovesi, J. Comput. Chem. **24**, 1305 (2003).
[64] J. Kushibiki, I. Takanaga, and S. Nishiyama, IEEE Trans. Ultrason. Ferroelectr. Freq. Control **49**, 125 (2002).
[65] H. Wang, B. Xu, X. Liu, J. Han, S. Shan, and H. Li, J. Cryst. Growth **79**, 227 (1986).
[66] Z. P. Chang, IEEE Trans. Sonics Ultrason. **SU-23**, 127 (1976).
[67] H. A. A. Sidek, G. A. Saunders, W. Hong, X. Bin, and H. Jianru, Phys. Rev. B **36**, 7612 (1987).
[68] D. S. Bailey, W. Soluch, D. L. Lee, J. F. Vetelino, J. Andle, and B. H. T. Chai, *Proceedings of the 36th Annual Frequency Control Symposium* (IEEE, New York, 1983), p. 335.
[69] W. Wallnöfer, P. W. Krempl, and A. Asenbaum, Phys. Rev. B **49**, 10075 (1994).
[70] G. F. Engel, P. W. Krempl, and J. Stadler, in *Proceedings of the Third European Frequency and Time Forum*, Besancon, 1989, edited by J. J. Gagnepain (ENSMM, Besancon, 1989), p. 50.
[71] F. Huard, Ph.D. thesis, Université des Sciences et Techniques du Languedoc, 1985.
[72] P. Armand, M. Beaurain, B. Ruffle, B. Menaert, D. Balitsky, S. Clement, and P. Papet, J. Cryst. Growth **310**, 1455 (2008).
[73] M. Mittal, S. L. Chaplot, A. I. Kolesnikov, C. K. Loong, O. D. Jayakumar, and S. K. Kulshreshtha, Phys. Rev. B **66**, 174304 (2002).
[74] P. Krempl, G. Schleinzer, and W. Wallnöfer, Sens. Actuators, A **61**, 361 (1997).
[75] R. M. Martin, Phys. Rev. B **9**, 1998 (1974).